AN ADVANCED ROBUST MIMO SSSC CONTROL TECHNIQUE FOR POWER OSCILLATION DAMPING IMPROVEMENT[*]

J. GHAISARI[**] AND A. BAKHSHAI

Dept. of Electrical and Computer Engineering, Isfahan University of Technology, Isfahan, I. R. of Iran
Email: ghaisari@electdp.iut.ac.ir
Dept. of Electrical and Computer Engineering, Queen's University, Kingston, Canada

Abstract– After a disturbance occurrence, fast damping of power oscillations is essential to reduce the risk of instability and thus increase the power transfer capacity of transmission systems. Recently, the Static Series Synchronous Compensator (SSSC) has justified its ability to improve power oscillation damping. Due to substantial interactions among the SSSC damping control loops and the power system variables, the use of conventional Single-Input Single-Output (SISO) control approaches results in a poor damping performance. In this paper, these interactions are taken into consideration, and a power system equipped with an SSSC is modeled as a multivariable system. The impact of the SSSC's dc voltage dynamic is also considered in the modeling. The power system equipped with an SSSC is multivariable with effective interactions among its variables. Traditional SISO control design techniques do not take into consideration these interactions and therefore cannot provide adequate damping over a wide range of operating conditions. Based on this developed multivariable modeling, a multivariable controller is proposed to improve power oscillation damping while keeping the dc-link voltage regulated. Simulation results verify the validity of the proposed modeling and control and show that the proposed approach can successfully damp out power system oscillations. Further simulation results show that the proposed controller provides a superior performance and a better robustness when compared to conventional SISO controllers.

Keywords– Power oscillation damping, SSSC, multivariable control, FACTS controllers

1. INTRODUCTION

Power oscillations are a common dynamic phenomenon which can affect a power system, partially or totally, after it has been subjected to a disturbance. Power oscillations, particularly in weak or long transmission lines, push the power system toward instability. To establish a reliable and secure power system, a large amount of the power transmission capacity is left unused as a power system stability margin. In other words, power system stability is achieved at the cost of excessive, but unused power transmission capability. An alternative to such a costly solution is to rapidly diminish the power oscillations by increasing the power system damping [1], [3]. Damping improvement is usually achieved by use of the Power System Stabilizer (PSS) [1], [2]. A traditional PSS, however, is a local compensating device and cannot damp out all oscillation modes. Nowadays, series FACTS controllers demonstrate superior and competitive features to improve Power Oscillation Damping (POD) [4]-[6]. Among these advanced solid-state series controllers are Thyristor Controlled Series Compensator (TCSC) [7]-[8] and Static Synchronous Series Compensator (SSSC) [9]-[11].

The SSSC, first initiated by Gyugyi *et al.* [12], injects a nearly sinusoidal and controllable voltage in

series with the transmission line. The main part of the SSSC is a Voltage Source Inverter (VSI) supplied by a dc-link capacitor. The injected voltage is perpendicular to the line current, and therefore emulates an inductive or a capacitive reactance in series with the transmission line, and influences the electric power flow in the line. The SSSC can improve POD by intelligent modulating of series reactive power compensation, and by absorbing the real power from or injecting it to the transmission line by means of its dc-link capacitor [13]. To achieve complete and acceptable damping performances, the series injected output voltage of the SSSC must be controlled quickly and accurately. In addition, the SSSC's dc-link voltage should be adjusted to allow VSI to work properly.

Control issues of the SSSC have been addressed by a number of individual researchers. In [14], two traditionally designed Single-Input Single-Output (SISO) PI controllers were employed to control the real and the reactive power flowing through a transmission line. In [9] the damping function of the SSSC, based on the linearized Phillips-Heffron model and SISO control structures, has been presented. In [10], an inverter-based series compensator was presented to damp power oscillation in a Single-Machine Infinite-Bus (SMIB) transmission system. In [10] a real-time simulation is used to adjust the coefficients of conventional PI controllers based on the linear model proposed in [11]. In the above mentioned research works, SISO controllers were traditionally designed using the classical control theory such as eigenvalue/eigenvector analysis, and root locus. In the SISO controller structures, the dynamic interactions among control loops are neglected. Thus, SISO controllers have not provided adequate damping over a wide range of operating condition variations [15], [16]. In addition, in most of these articles the dc link voltage dynamic is ignored. This could turn into a serious problem, especially when the compensator exchanges active power with the transmission system. In [15] a Multi-Input Multi-Output (MIMO) controller is designed to control the flow of power in a transmission line equipped by an SSSC.

In this paper, a multi-functional SSSC is employed to improve the power oscillation damping in a SMIB power system. Considerable interactions among the SSSC control variables and power system variables are taken into consideration, and the dc-link voltage dynamic is not ignored. For the sake of clarity and for better understanding of the proposed control approach, and without limiting the generality, the power system is referred by a simple SMIB model. Accordingly, a multivariable model for the SMIB power system equipped with an SSSC is developed, and a multivariable controller is designed. The proposed multivariable controller design is based on the diagonal dominance approach, also called the Parameterized Pre-Compensator technique. A change in the power demand usually causes electromechanical and power oscillations. Thus, in this paper, the disturbance is modeled by a step change in the mechanical input torque of the generator. Simulations are carried out in PSCAD/EMTDC. Simulation results verify the validity of the proposed MIMO controller and its excellent performance in improving power oscillation damping, as well as adjusting the dc-link voltage. To show the superiority of the proposed MIMO controller over the conventional SISO controllers, simulation results from both techniques are compared. Also, it is shown that the proposed MIMO controller considerably increases the system robustness when compared to its SISO counterpart controllers.

2. SSSC MODELING

Figure 1 shows a single line diagram of an SMIB power system equipped with a Static Series Synchronous Compensator (SSSC). The SSSC injects a series controlled voltage, V_{pq}, into the transmission line. The magnitude and the phase angle of this voltage can be controlled to achieve better system capacity and performance. As shown in Fig. 1, the SSSC consists of a Voltage Source Inverter (VSI), a dc-link capacitor, and a series transformer.

The SSSC is modeled by a loss-less VSI, an ideal transformer, a dc-link capacitor, and a shunt

resistor, r_p, representing all power losses including inverter switches and conduction losses, and the electrical and magnetic losses of the transformer. The transmission line is modeled by a lumped inductance in series with a resistance representing the line losses, and the generator is modeled by means of a simplified second order dynamic equation [1].
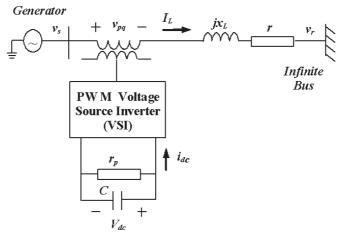

Fig. 1. An SSSC installed in a SMIB three-phase transmission system

By means of the time varying p-q transformation given in (1)

$$C = \frac{2}{3} \begin{bmatrix} \frac{1}{\sqrt{2}} & \frac{1}{\sqrt{2}} & \frac{1}{\sqrt{2}} \\ Cos\theta & Cos(\theta - \frac{2\pi}{3}) & Cos(\theta + \frac{2\pi}{3}) \\ Sin\theta & Sin(\theta - \frac{2\pi}{3}) & Sin(\theta + \frac{2\pi}{3}) \end{bmatrix} \tag{1}$$

'abc' quantities are transferred to a *'pq0'* frame. The p-axis is always coincident with the instantaneous generator internal phase voltage, and the q-axis in quadrature with it. Figure 2 shows the voltage and current vectors when transferred to the p-q reference frame. Voltage harmonics are neglected in this diagram. The output voltage of the SSSC is shown in Fig. 2 for both capacitive and inductive modes.
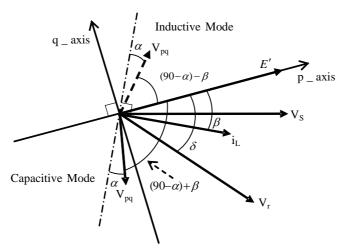

Fig. 2. The phasor diagram of the output voltage of the SSSC for both capacitive and inductive modes

Dynamic equations governing the behavior of the system in a per unit system are obtained and given by (2)

$$\frac{d}{dt}i_p = -\frac{r\omega_s}{x_e}i_p + \omega_1 i_q + \frac{\omega_s}{x_e}\left(\left|E'\right| - v_{rp} - v_p\right)$$

$$\frac{d}{dt}i_q = -\omega_1 i_p - \frac{r\omega_s}{x_e}i_q + \frac{\omega_s}{x_e}\left(-v_{rq} - v_q\right) \qquad (2)$$

$$\frac{d}{dt}\omega = \frac{1}{M}(T_m - T_e - D\omega) \qquad (p.u.)$$

$$\frac{d}{dt}\delta = \omega_s(\omega - 1) \qquad (rad/\sec)$$

where variables and parameters are defined as follows (all in p.u., except where indicated):

i_L :   Line current.

i_p :   Component of the line current coincident with the p-axis.

i_q :   Component of the line current coincident with the q-axis.

V_{dc} :   SSSC's dc-link voltage.

δ :   Power angle in rad.

ω :   Rotor angular speed.

ω_s :   Synchronous angular frequency in rad/s.

ω_1 : $\omega_s \times \omega$.

r :   Line equivalent resistance.

x_e :   Total inductance of the transmission system.

x_c :   DC-link reactance.

r_p :   Fictitious resistance representing the inverter losses.

E' :   Generator phase e.m.f behind the transient reactance.

V_s :   Generator terminal voltage.

v_{rp}, v_{rq} :   Components of the infinite-bus voltage in coincident with the p-axis and q-axis respectively.

V_{pq} :   SSSC injected series voltage.

v_p, v_q :   Components of V_{pq} in coincident with the p-axis and q-axis respectively.

T_m :   Input mechanical torque.

T_e :   Electromagnetic torque.

M :   Generator's moment of inertia.

D :   Rotational damping.

k :   Ratio of the fundamental output voltage peak to the dc voltage of the SSSC.

α :   Angle deviation of the VSI output voltage measured from its ideal form that is perpendicular to the line current.

Ideally, the injected voltage, V_{pq}, is perpendicular to the line current. However, to compensate for the inverter losses and to keep the dc voltage constant, the injected voltage is slightly shifted from its ideal quadrature form. By using Fig. 2, components of the injected voltage, v_p and v_q, are obtained in the capacitive and the inductive modes separately. They are given in the capacitive mode by (3):

$$v_p = kV_{dc}\sin(\beta - \alpha) = kV_{dc}(\sin\beta\cos\alpha - \cos\beta\cdot\sin\alpha) \qquad (3)$$

$$v_q = kV_{dc}\cos(\beta - \alpha) = kV_{dc}(\cos\beta\cos\alpha + \sin\beta\cdot\sin\alpha)$$

and in the inductive mode by (4):

$$v_p = kV_{dc}\sin(\beta + \alpha) = kV_{dc}(\sin\beta\cos\alpha + \cos\beta\cdot\sin\alpha) \qquad (4)$$

$$v_q = kV_{dc}\cos(\beta + \alpha) = kV_{dc}(\cos\beta\cos\alpha - \sin\beta\cdot\sin\alpha)$$

where k is the ratio of the fundamental output voltage peak to the dc voltage of the SSSC, and is proportional to the modulation index of the PWM inverter. α is the angle deviation of the inverter's output voltage measured from its ideal form that is perpendicular to the line current, and $\beta = -\tan^{-1}(\frac{i_q}{i_p})$ is the phase angle of the line current.

The infinite-bus voltage coincident with the p-axis, v_{rp}, and the q-axis, v_{rq}, are obtained easily as:

$$
\begin{aligned}
v_{rp} &= \left|V_r^\infty\right|\cos\delta \\
v_{rq} &= \left|V_r^\infty\right|\sin\delta
\end{aligned}
\tag{5}
$$

To analyze the impact of the dc-link voltage on the SSSC performances, the dynamic of the dc-link voltage should also be considered. Since the total loss of the SSSC is represented by r_p, the VSI in Fig. 1 is ideal, and the average power at the dc and ac terminals of such an ideal inverter are equal. That means $P_{dc\_ave} = P_{ac\_ave}$. The average active power in the ac side of the inverter in terms of the '$pq0$' variables is given by (6)

$$
P_{ac\_ave} = \frac{3}{2}(v_p i_p + v_q i_q + v_0 i_0)
\tag{6}
$$

By substitution of (3) or (4) in (6) and some mathematical calculations, P_{ac_ave} is obtained as:

$$
P_{ac\_ave} = \frac{3}{2}\sqrt{i_p^2 + i_q^2}\, k V_{dc} \sin\alpha
\tag{7}
$$

Since $P_{dc\_ave} = P_{ac\_ave}$, by using $P_{dc\_ave} = V_{dc}i_{dc}$ and (7) the following expression is achieved as:

$$
i_{dc} = \frac{3}{2}\sqrt{i_p^2 + i_q^2}\, k \sin\alpha
\tag{8}
$$

Also, the dc side voltage dynamic in per unit base is given by

$$
\frac{d}{dt}V_{dc} = -\omega_s x_c\left(i_{dc} + \frac{1}{r_p}V_{dc}\right)
\tag{9}
$$

Substituting i_{dc} from (8) into (9) gives the dynamic equation of the dc-link voltage as:

$$
\frac{d}{dt}V_{dc} = -\frac{3}{2}\omega_s x_c\sqrt{i_p^2 + i_q^2}\, k \sin\alpha - \frac{\omega_s x_c}{r_p}V_{dc}
\tag{10}
$$

Equations (2) and (10) give the mathematical model of an SMIB power system equipped with an SSSC. This model is represented by a standard multivariable nonlinear dynamic system equation given by (11)

$$
\dot{x} = f(x, u_{pwm})
\tag{11}
$$

where $x = [x_1, x_2, x_3, x_4, x_5]^T = [i_p, i_q, V_{dc}, \omega, \delta]^T$, and $u_{pwm} = [k, \alpha]^T$.

To design a controller for power oscillation damping improvement and the dc-link voltage adjustment, the output of the system is defined as:

$$y = \begin{bmatrix} x_4 \\ x_3 \end{bmatrix} = \begin{bmatrix} \omega \\ V_{dc} \end{bmatrix} \tag{12}$$

$x_4 = \omega$ is the rotor angular speed (in *p.u.*), in which deviation from its nominal value (1 p.u.) alerts the existence of low frequency power oscillations [1], and $x_3 = V_{dc}$ is the dc-link voltage. The dc-link can exchange active power with the power transmission line, and therefore can improve power oscillation damping.

To obtain a linear multivariable model, the nonlinear model specified in (11) is linearized at a stable operating point. The parameters of the power system, as well as the operating point, X_{o1}, used in this paper, are given in the appendix. The linearized multivariable system is calculated and obtained as:

$$\dot{x} = Ax + Bu \tag{13}$$
$$y = Cx + Du$$

where

$$A = \begin{bmatrix} 8.7425 & 350.26 & -384.74 & -565.02 & 1104.9 \\ -326.19 & -32.941 & -666.39 & -978.64 & 1016 \\ 0.0 & 0.0 & -1.2566 & 0.0 & 0.0 \\ -0.37485 & 0.0 & 0.0 & -0.37485 & 0.0 \\ 0.0 & 0.0 & 0.0 & 314.1530 & 0.0 \end{bmatrix}, \ B = \begin{bmatrix} 119.4 & -149.94 \\ -206.81 & -86.566 \\ 0.0 & -49.156 \\ 0.0 & 0.0 \\ 0.0 & 0.0 \end{bmatrix}$$

$$C = \begin{bmatrix} 0.0 & 0.0 & 0.0 & 1.0 & 0.0 \\ 0.0 & 0.0 & 1.0 & 0.0 & 0.0 \end{bmatrix}, \text{ and } D = \begin{bmatrix} 0.0 & 0.0 \\ 0.0 & 0.0 \end{bmatrix}$$

It can easily be shown that the controllability matrix, $[B \ AB \ A^2B \ A^3B \ A^4B]$, is a full rank matrix and the pair (A, B) is controllable [17]. Thus, there exist control signals, k and α, which can steer the system from any initial state to any desired final state in a finite time interval.

3. MULTIVARIABLE CONTROLLER DESIGN

In this section, a multivariable PI controller based on a diagonal dominance approach, called Parameterized Pre- Compensator [18], is proposed. It will be demonstrated that a unified MIMO controller can successfully be designed for the SSSC to improve power oscillation damping in addition to regulating the dc-link voltage. The block diagram of the multivariable controller for the SSSC installed in the power system is shown in Fig. 3.
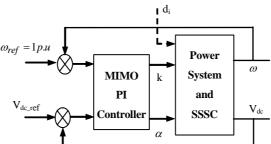
Fig. 3. MIMO control system block diagram

The multivariable PI control law is presented by

$$\begin{bmatrix} k \\ \alpha \end{bmatrix} = (K_P + \frac{1}{s} K_I) \begin{bmatrix} \omega_{ref} - \omega \\ V_{dcref} - V_{dc} \end{bmatrix}, \ K_P, K_I \in R^{2 \times 2} \tag{14}$$

Parameters of the multivariable PI controller can be set by means of standard design methods for

multivariable control systems. In this research a method based on the parameterized pre-compensation approach is applied.

The parameterized pre-compensation is a MIMI controller design method that minimizes the interactions between input-output pairs of multivariable systems [18]. The column dominance measure is a means to specify interactions in a multivariable system, and is defined for the jth column of a system transfer function as:

$$d_j^c(Q(j\omega)) = \sum_{\substack{i=1 \\ i \neq j}}^{m} \frac{|q_{ij}(j\omega)|}{|q_{jj}(j\omega)|} \tag{15}$$

where $Q(j\omega) \in C^{m \times n}$ is the open loop transfer function of the system.

Consider a typical feedback control system shown in Fig. 4. By means of a parameterized pre-compensation approach, the controller, $K(s)$, should be designed in such a way that the column dominance measure of the compensated system, $Q(s) = G(s)K(s)$, is minimized. The stability of the compensated system is guaranteed by dominance theorems [18]. In addition, satisfactory performance of the system can be achieved by selecting a proper structure for $K(s)$. In this research work, $K(s)$ is a MIMO PI controller with a control law defined by (14). The matrix transfer function of the power system equipped with the SSSC is derived from (13) and given by (16).

$$G(s) = \frac{1}{s^5 + 25.83\,s^4 + (1.1379 \times 10^5)s^3 + (1.8032 \times 10^5)s^2 + (4.6239 \times 10^7)s + (5.8047 \times 10^7)} \times$$

$$\begin{bmatrix} -44.758s^3 - 25623s^2 - 32269s & 56.206s^3 + 6198.5s^2 - (4.5178 \times 10^6)s \\ 0.0 & -49.156s^4 - 1208s^3 - (5.5921 \times 10^6)s^2 - (1.8368 \times 10^6)s - 2.2706 \times 10^9 \end{bmatrix} \tag{16}$$

Fig. 4. A typical feedback control system

Now, let $s = j\omega$

$$\begin{aligned} Q(j\omega) &= G(j\omega)K(j\omega) \\ &= [G_R(j\omega) + jG_I(j\omega)][K_P + \frac{1}{j\omega}K_I] \\ &= [G_R(j\omega)K_P + \frac{1}{\omega}G_I(j\omega)K_I] + j[G_I(j\omega)K_P - \frac{1}{\omega}G_R(j\omega)K_I] \\ &= [\overline{G}_R(j\omega) + j\overline{G}_I(j\omega)]\overline{K} = \overline{G}(j\omega)\overline{K} \end{aligned} \tag{17}$$

where G_R and G_I are the real and the imaginary parts of $G(j\omega)$, respectively. The real and the imaginary part of the modified system, $\overline{G}(j\omega)$, are defined in (18):

$$\overline{G}_R(j\omega) = [G_R(j\omega), \frac{1}{\omega}G_I(j\omega)] \in C^{2\times4}, \text{ and } \overline{G}_I(j\omega) = [G_I(j\omega), -\frac{1}{\omega}G_R(j\omega)] \in C^{2\times4} \tag{18}$$

and the modified controller is $\overline{K} = [K_p, K_I]^T \in R^{4\times2}$.

By means of Eqs. (17) and (18), the problem of finding $K(s) \in C^{2\times2}$ for the system $G(s)$ is cut down to finding $\overline{K} \in R^{4\times2}$ for the modified system $\overline{G}(s)$. The jth column dominance measure of the compensated system, $Q(s) = \overline{G}(s)\overline{K}(s)$, is defined by

$$d_j^c(Q(j\omega)) = \sum_{\substack{i=1\\i\neq j}}^2 \frac{\left|q_{ij}(j\omega)\right|}{\left|q_{jj}(j\omega)\right|} = \sum_{\substack{i=1\\i\neq j}}^2 \frac{\left|\overline{g}_i(j\omega)\overline{k}_j\right|}{\left|\overline{g}_j(j\omega)\overline{k}_j\right|} \tag{19}$$

where $\overline{g}_i$ is the row vector of $\overline{G}$ and $\overline{k}_j$ is the column vector of $\overline{K}$.

Equation (19) shows that the jth column dominance measure of Q(s) depends only on the jth column of $\overline{K}$. Therefore, the minimization measures of finding $\overline{K}$ are reduced to some simpler minimization steps. In such simplified procedures, each step only involves finding one column of $\overline{K}$. The minimization measure of finding a column vector $\overline{k}_j$ is given by

$$P_j : \min_{k_j \in S} \ \max_{\omega} d_j^c(Q(j\omega)) \tag{20}$$

The set S represents the various constraints on $\overline{K}$. Particularly, in the MIMO controller given in (15), all components of K_P and K_I should be positive. The min-max problem, P_j, can be solved using well-known methods such as linearly constrained min-max optimization [19]. In this paper, an indirect method based on the feasible set [18] is used to solve the optimization problem, P_j. By solving the optimization problem given by (20) for P_j, $j = 1,2$, $\overline{K}$ is calculated and then K_P and K_I are obtained

$$K_P = \begin{bmatrix} 0.18 & 17.2 \\ 0.0 & 28.5 \end{bmatrix}, \text{ and } K_I = \begin{bmatrix} 0.005 & 5016.0 \\ 0.00 & 0.01 \end{bmatrix} \tag{21}$$

4. SISO CONTROLLER DESIGN

To compare the performance and robustness of the proposed MIMO controller with those of the conventional SISO control structures, in this section two separate standard Single-Input Single-Output (SISO) PI controllers are designed. The block diagram of the SISO controllers is shown in Fig. 5. Two PI controllers, one for damping the power oscillation and the other for regulation of the dc voltage, are used.

The controllers' dynamics are given by

$$k = (K_{p\omega} + \frac{1}{s}K_{i\omega})(\omega_{ref} - \omega), \text{ and } \alpha = (K_{pdc} + \frac{1}{s}K_{idc})(V_{dcref} - V_{dc}) \tag{22}$$

PI Controllers are adjusted by means of a PI standard tuning method [20]. Parameters of PI controllers are calculated at the operating point, X_{o1}, given in the appendix. The calculated controllers' gains are $K_{p\omega} = 0.15$, $K_{i\omega} = 0.002$, $K_{pdc} = 15.0$, and $K_{idc} = 0.4$.
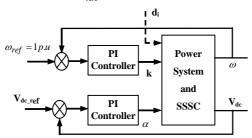

Fig. 5. SISO control system block diagram

5. SIMULATION RESULTS

Real time simulations are carried out in a PSCAD/EMTDC environment. A 600 MVA synchronous generator is connected to a 230 kV three-phase ac transmission line via a Y/Δ transformer. The SSSC is built by a 60 MVA power converter. The power converter is connected in series at the sending end of a

transmission line by a Δ/Y transformer. The dc-link voltage is set to be 40 kV at steady state operation. The proposed parameterized pre-compensator MIMO PI controller is used to simultaneously damp power oscillation and adjust the dc-link voltage after a disturbance has arisen. Their alternatives, SISO PI controllers that were designed in the previous section, are also simulated to show the superiority of the MIMO controller performance. Disturbance is realized by applying a step change in the generator mechanical input torque. Simulation results performed in PSCAD for both MIMO and SISO controllers are depicted in Figs. 6-12.
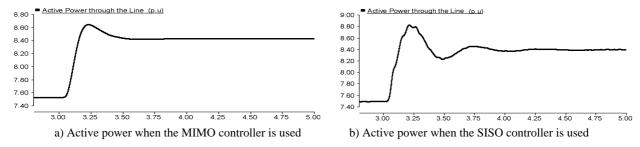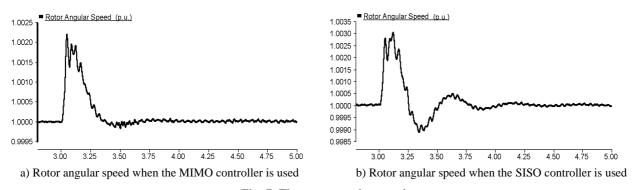
a) Active power when the MIMO controller is used   b) Active power when the SISO controller is used

Fig. 6. The active power transmitted through the line

a) Rotor angular speed when the MIMO controller is used   b) Rotor angular speed when the SISO controller is used

Fig. 7. The rotor angular speed

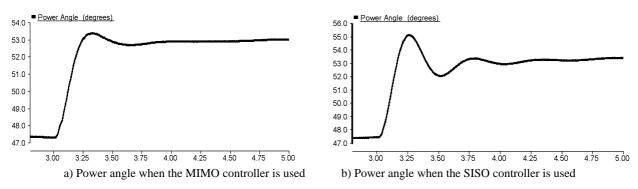a) Power angle when the MIMO controller is used   b) Power angle when the SISO controller is used

Fig. 8. The power angle in degrees

a) DC link voltage when the MIMO controller is used   b) DC link voltage when the SISO controller is used
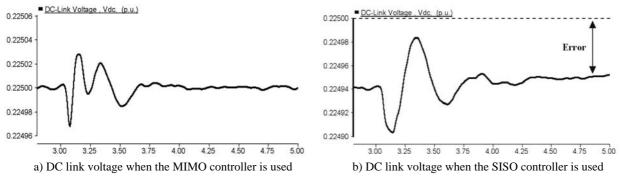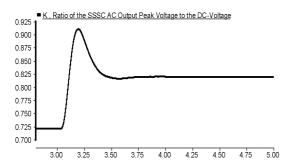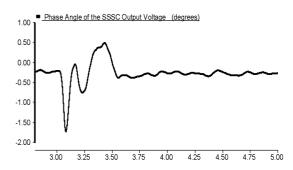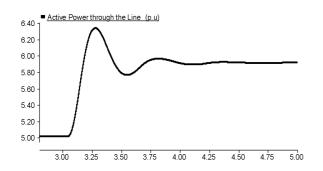
Fig. 9. The dc-link voltage of the SSSC

a) The ratio of the ac output peak voltage to the dc voltage of the SSSC   b) The angle deviation of the VSI output voltage
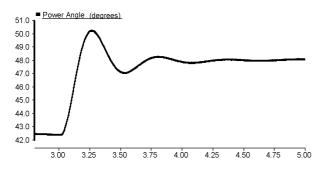
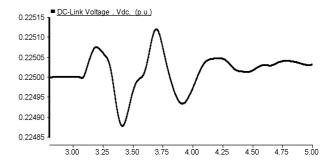Fig. 10. Control signals k and α when the proposed MIMO controller is used

a) The active power transmitted from the line   b) The rotor angular speed achieved by MIMO controller
achieved by MIMO controller

c) The power angle in degrees achieved by MIMO controller   d) The dc-link voltage of the SSSC achieved
by MIMO controller

Fig. 11. Simulation results achieved by means of proposed MIMO controller when
the operating point is changed

In all figures, the horizontal axes depicts time (in seconds), and the vertical axes show per unit values, per-unitized based on the phase nominal variables, except those that are indicated.

a) Step change in the generator input torque

The proposed MIMO controller and its counterpart SISO controller, which are designed in previous sections for the operating point, X_{o1} given in the appendix, are separately employed to control the SSSC and to improve power oscillation damping. At $t = 3 \sec$, a step change is applied to the generator input torque and consequential simulation results are obtained for both controllers.

Figure 6 shows the step responses of the active power transmitted through the line for both controllers. It can be seen that the proposed MIMO controller significantly improves the power oscillation damping in comparison with the SISO controller. The MIMO controller diminished the overshoot from 50% in the SISO controller response, to 25%. The smaller overshoot in the power transmitted response

justifies the use of a smaller stability margin. Therefore, the transmission capacity can be increased securely.

a) The active power transmitted from the line
obtained by SISO controller

b) The rotor angular speed obtained
by SISO controller

c) The power angle in degrees obtained by SISO controller

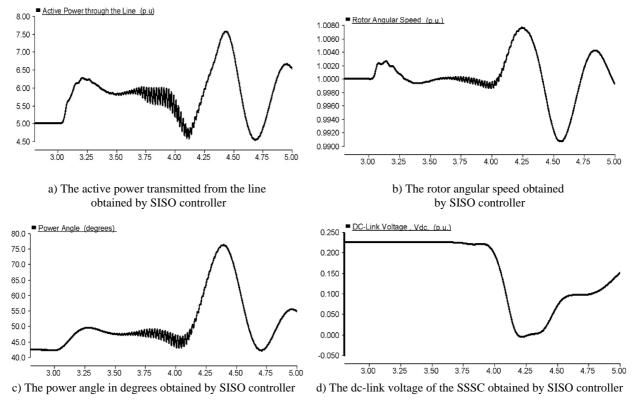d) The dc-link voltage of the SSSC obtained by SISO controller

Fig. 12. Simulation results obtained by means of SISO controllers when the operating point is changed

Figure 7 demonstrates the generator angular speed for both the MIMO and SISO controllers. However both controllers can keep the generator angular speed at $\omega = 1\,p.u.$, and after a deviation, the proposed MIMO controller illustrates faster and better performance, as well as smaller deviation from its nominal value.

The power angle is shown in Fig. 8. It can be seen that the MIMO controller effectively damps the power angle oscillations and reduces the overshoot to 7.0%. The overshoot is about 36.3% when the SISO controllers are used. Actually, the power angle represents the rotor angular position of the generator. Effective and fast damping performance achieved by the proposed MIMO controller decreases the risk of the generator instability.

Figure 9 shows the dc-link voltage in two cases. Both MIMO and SISO controllers regulate the dc-link voltage, however the SISO controller creates a steady state error to reach $V_{dc\_ref} = 0.22500\,(p.u.)$ shown in Fig. 9b. The SISO PI controller is designed to achieve the zero steady state error when no interaction among the control loops is assumed. This incorrect assumption causes a deviation in the simulated results. In the proposed multivariable controller design, however, these interactions are taken into consideration, and thus the dc-link voltage error is zero, and the dc side voltage is regulated at steady state. Also, the maximum error occurred by the MIMO controller is smaller than those of the SISO controller.

Figure 10 demonstrates the control signals k and α when the MIMO controller is used. It is clear that the proposed MIMO controller satisfies practical constraints such as $0 < k \leq 1$, and $-90^\circ \leq \alpha \leq 90^\circ$.

b) Robustness performance

To investigate robustness of the MIMO controller and to show its superiority over the conventional

SISO controllers, both are employed to control the SSSC when the operating point of the power system is changed from X_{o1}, used to design the controllers, to the new operating point, X_{o2} given in appendix. Simulation results are obtained for both the MIMO and SISO controllers separately and depicted in Figs. 11 and 12 respectively. It is clearly seen that the proposed MIMO controller remains stable and shows excellent robustness and performance in the new operation condition, while the SISO controllers become unstable and fail to control the SSSC when the operating point is changed.

Actually, the SSSC is a multifunctional FACTS controller with effective interactions among its control loops, which have very important roles in the SSSC performance and robustness. These interactions are taken into account when the multivariable model is achieved and the MIMO controller is designed. On the other hand, in conventional SISO, controller interactions among control loops are ignored.

6. CONCLUSION

Static Synchronous Series Compensator (SSSC) is progressively being used to enhance power oscillation damping in power systems. In this paper, a multivariable model for a power system equipped with an SSSC is developed. This multivariable model describes the dynamic behavior of the power system equipped with the SSSC more precisely. A multivariable controller is designed based on this model, and based on the principles of the parameterized pre-compensation approach. The proposed multivariable controller can successfully damp power oscillations as well as regulate the dc link voltage. In the controller design procedure, couplings among control loops are also minimized.

Simulation results, carried out in a PSCAD/EMTDC environment, show the viability of the developed system model and the proposed controller. Simulation results also justify the superiority of MIMO techniques over the SISO approaches in enhancing power oscillation damping as well as the dc-link voltage regulation. In addition, the proposed MIMO controller performs more robustly when the operating conditions are changed. Fast diminishing power oscillation allows the secure use of more line capacity and therefore increases the power transfer capacity of the transmission system.

REFERENCES

1. Kundur, P. (1994). *Power System Stability and Control.* New York, McGraw-Hill.
2. Gibbard, M. J. (1991). Robust design of fixed-parameter power system stabilizers over a wide range of operating conditions. *IEEE Trans. on Power Systems, 6*(2), 794-800.
3. de Mello, F. P. (1994). Exploratory concepts on control of variable series compensation in transmission systems to improve damping of inter-machine system oscillations. *IEEE Trans. on Power Systems, 9*(1), 102- 108.
4. Noroozian, M., Ghandhari, M., Andersson, G., Gronquist, J. & Hiskens, I. (2001). A robust control strategy for shunt and series reactive compensators to damp electromechanical oscillations. *IEEE Trans. on Power Delivery,16*(4), 812-817.
5. Chen, X. R., Pahalawaththa, N. C., Annakkage, U. D. & Kumble, C. S. (1995). Controlled series compensation for improving the stability of multi-machine power systems, *IEE Proc. Gener. Transm. Distrib., 142*(4), 361-366.
6. Chen, J., Lie, T. T. & Vilathgamuwa, D. M. (2003). Enhancement of power system damping using VSC-based series connected FACTS controllers. *IEE Proc. Gener. Transm. Distrib., 150*(3), 353-359.
7. Chaudhuri, B. & Pal, B. C. (2004). Robust damping of multiple swing modes employing global stabilizing signals with a TCSC. *IEEE Trans. on Power Systems, 19*(1), 499- 506.

8. Son, K. M. & Park, J. K. (2000). On the robust LQG control of TCSC for damping power system oscillations. *IEEE Trans. on Power Systems, 15*(4), 1306- 1312.

9. Wang, H. F. (1999). Design of SSSC damping controller to improve power system oscillation stability. *AFRICON, 1999 IEEE, 1*, 495–500.

10. Kazemi, A., Ladjevardi, M. & Masoum, M. S. (2005). Optimal selection of SSSC based damping controller parameters for improving power system dynamic stability using genetic algorithm. *Iranian Journal of Science and Technology, Transaction B, 29*(B1), 1-10.

11. Swift, F. J. & Wang, H. F. (1996). Application of the controllable series compensator in damping power system oscillations. *IEE Proc. Gener. Transm. Distrib., 143*(4), 359-364.

12. Gyugyi, L., Schauder, C. D. & Sen, K. K. (1997). Static synchronous series compensator: a solid-state approach to the series compensation of transmission lines. *IEEE Trans. on Power Delivery, 12*(1), 406-417.

13. Hingorani, M. G. & Gyugyi, L. (1999). *Understanding FACTS: concepts and technology of Flexible AC Transmission Systems,* IEEE Press, New York.

14. Papic, I. & Gole, A. M. (2001). Enhanced control system for a static synchronous series compensator with energy storage. in *Proc. 2001 IEE Conference* on *AC-DC Power Transmission,* Conf. Publ. No. 485, 327-332.

15. Ghaisari, J. & Bakhshai, A. (2004). Parameterize pre-compensator design for Static Synchronous Series Compensator (SSSC). in *Proc. 2004 IEEE Canadian Conference on Electrical and Computer Engineering, CCECE 2004, 3*, 1617-1620.

16. Wang, H. F. & Wu, W. H. (2000). Multivariable design of a multiple-functional unified power flow controller. *Power Engineering Society Summer Meeting, 2000. IEEE, 3*, Seattle, USA, 1363-1368.

17. Shinners, S. M. (1998). *Modern Control System Theory and Design,* 2nd Edition, New York, John Wiley and Sons Inc.

18. Bryant, G. F. & Yeung, L. F. (1996). *Multivariable control system design techniques,* New York, John Wiley and Sons Inc.

19. Madsen, K. & Jacobsen, H. S. (1978). Linearly constrained min-max optimization. *Mathematical Programming,* Springer, *14*(1), 208-223.

20. Astrom, K. J. & Wittenmark, B. (1984). *Computer controlled systems: Theory and Design,* Prentice-Hall.

APPENDIX

The parameters of the synchronous machine, the transmission system and the SSSC are (all in p.u., except where indicated):

$X'_d = 0.046$, $R_a = 4.243 \times 10^{-4}$, $\omega_s = 100\pi$, $H = 3.22$, $X_t = 0.10$, $X_L = 0.15$, $T'_{d0} = 8.0 \sec$, $D = 0$, $x_c = 0.04$, $R_L = 1.10 \times 10^{-2}$, $r_p = 10$, $|V_s| = 1.0$, and $V_{dc} = 0.225$.

The operating point, X_{o1}, used for the simulations is:

$$X_{01} = \begin{bmatrix} 3.1151 & -1.7985 & 0.225 & 1.00 & 0.8273 \end{bmatrix}^T.$$

The second operating point, X_{o2}, which is used for robustness investigation in section *V.B* and Figs. 11-12, is:

$$X_{o2} = \begin{bmatrix} 2.357 & -0.9908 & 0.225 & 1.00 & 0.7400 \end{bmatrix}^T.$$